International Journal of QUANTUM CHEMISTRY

Theoretical Prediction for the Structures of Gas Phase Lithium Oxide Clusters: $(Li_2O)_n$ (n = 1–8)

Yuan Yuan and Longjiu Cheng*

We apply genetic algorithm combining directly with density functional method to search the potential energy surface of lithium-oxide clusters $(Li_2O)_n$ up to $n = 8$. In $(Li_2O)_n$ (n = 1–8) clusters, the planar structures are found to be global minimum up to $n = 2$, and the global minimum structures are all three-dimensional at $n \geq 3$. At $n \geq 4$, the tetrahedral unit (TU) is found in most of the stable structures. In the TU, the central Li is bonded with four O atoms in sp^3 interactions, which leads to unusual charge transformation, and the probability of the central Li participating in the bonding is higher by adaptive natural density partitioning analysis, so the central Li is in particularly low positive charge. At large cluster size, distortion of structures is viewed, which breaks the symmetry and may make energy higher. The global minimum structures of $(Li_2O)_2$, $(Li_2O)_6$, and $(Li_2O)_7$ clusters are the most stable magic numbers, where the first one is planar and the later both have stable structural units of tetrahedral and C_{4v}. © 2012 Wiley Periodicals, Inc.

DOI: 10.1002/qua.24274

Introduction

Clusters are microscopic or submicroscopic aggregates which are composed of several to hundreds of atoms or molecules. Because of the outstanding physical and chemical properties, studies on clusters have gradually evoked great interest in recent years. Research on cluster is developing rapidly, which is an interdisciplinary of atomic physics, molecular physics, solid state physics, surface physics, quantum chemistry, and many other disciplines.[1] As clusters have excellent catalytic properties, biological activity, optical properties, superconducting properties, and so forth, most countries make clusters as focus of researches, especially, the nano-clusters. With the continuous development of cluster theory, optimization of the structure of clusters can not only reveal law of the changes for structures in the growth of clusters but also can find the formation mechanism and conditions of the structures of cluster-specific. Through predicting the structure of cluster can guide to experiment further, improve the conditions and provide a theoretical basis for the design and development of new materials.

At present, many advances have been done in understanding of metallic and semiconductor clusters, the study of metal-oxide clusters plays a fundamental role in many physical and chemical processes. In recent years, some studies have been done on metal-oxide clusters, such as magnesium-oxide (MgO),[2–6] calcium-oxide (CaO),[7,8] barium-oxide (BaO),[9–12] cesium-oxide (Cs_2O),[13,14] silicon-oxide (Si_2O),[15–19] titanium-oxide (Ti_2O),[16,20–22] zirconia (ZrO_2),[20,23–25] lithium-oxide (Li—O),[26–29] and so forth. In particular, small clusters of lithium-oxide can attract more interest. In 1993, Bréchignac et al.[26] studied nonstoichiometric lithium-oxide clusters (Li_nO_m, $0 \leq n \leq 10$, $0 \leq m \leq 6$) and made a conclusion that the odd–even oscillations which are generally seen in abundance spectra and ionization potentials in metallic clusters, progressively weaken and vanish when the oxygen content increases. Then, in 1996, Finocchi and Noguera[27] studied ground-state properties of stoichiometric lithium-oxide clusters ($Li_{2n}O_n$, n = 2, 3, 4, 6) by means of *ab initio* molecular-dynamics simulations, in conjunction with a global optimization strategy. They found several stable isomers for each cluster size and presented a remarkable variety of bonding configurations. In the conclusion, they shown that it is possible to characterize the global bonding properties of a $Li_{2n}O_n$ cluster at given size despite the structural differences among the various isomers. Next, in 1997, Finocchi et al.[28] applied density functional theory (DFT) to calculate the electronic structure. In 2005, Viallon et al.[29] studied electronic properties of mixed lithium-oxide clusters by experimental methods.

Li_2O crystallizes in the antifluorite structure (Fig. 1) with a face-centered cubic lattice and belongs to the Fm3m (O_h^5) space group,[30] lithium being in the tetrahedral coordination. The structure of crystal Li_2O is different from $(Li_2O)_n$ cluster completely.

Geometric global optimization is to determine the structural organization for a set of atoms that minimizes the total potential energy by searching the whole potential energy surface (PES), which is a nondeterministic polynomial-time-hard problem. Determining the lowest energy structures is an important piece of information, which can help in understanding the properties. Lithium-oxide cluster is the most simple metal-oxide cluster. However, searching the *ab initio* PES of

Y. Yuan, L. Cheng
School of Chemistry and Chemical Engineering, Anhui University, Hefei, Anhui, 230039, P. R. China
E-mail: clj@ustc.edu

Contract grant sponsors: 211 Project and Outstanding Youth Foundation of Anhui University.
Contract grant sponsor: National Natural Science Foundation of China; contract grant number: 20903001.

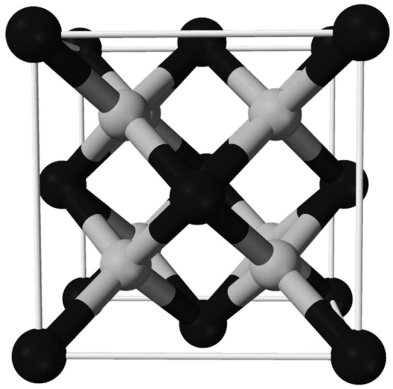

Figure 1. The crystal structure of lithium oxide, Li black, O light gray.

lithium-oxide clusters is still of great challenging even at small cluster size. In some binary clusters, such as $(BN)_n$ and $(MgO)_n$ in ratio of 1:1, the structures can be easily modeled with certain growth patterns. $(Li_2O)_n$ clusters are in ratio of 2:1, so the growth patterns are irregular and the structures are often unexpected and cannot be modeled.

Because of the difficulty in determining the global minimum structures, although some theoretical and experimental works have been done as mentioned above, the structural features of lithium-oxide cluster and how the structure changes as the size increases are still not so clear. Therefore, in this work, we perform an unbiased global search of the *ab initio* PES of $(Li_2O)_n$ clusters up to $n = 8$ using genetic algorithm (GA) combined directly with DFT method. The other groups performed global optimization of Si_n[31] and $HCl(H_2O)_n$[32] clusters using Monte Carlo approaches directly at the DFT level. The GA-DFT method was also applied to search the PES of Ag_n,[33] Li_n,[34] and $(TiO_2)_n$[22] clusters. As the smallest metal-oxide cluster, lithium-oxide cluster can act as a benchmark, so the study of lithium-oxide cluster also has some significance.

Computational Details

Global optimization method

To have a systemic study of $(Li_2O)_n$ clusters, GA was applied to search the PES with DFT method. All DFT computations were completed by the GAUSSIAN 09 package.[35] Our cluster GA-DFT method can be summarized as follows:

a Generate *npop* structures randomly to form the starting population of GA. Relax each structure in the population by DFT method at the B3LYP/3-21G[36–38] level with a loose convergence criterion (10^{-3} Hartree in the total energy, 0.0017 Hartree/Å for the force, and 0.0067 Å for the displacement).

b For *k*th iteration, choose two structures from the population randomly and perform Deaven-Ho crossover[39] operation to generate one child structure. After mutation operation, relax the child structure by DFT method at the B3LYP/3-21G level with a loose convergence criterion. Input the relaxed structure to the structural bank. Update the population based on similarity[40] and energy.

c Increase *k* by 1. If *k* reaches a presetting number, terminate current calculation. Otherwise, go to step b).

Because GA cannot promise to find the global minimum structure in one calculation, for each case, five independent GA runs are carried out and the relaxed structures are recorded in one structural bank. Only small basis set can be used by global search procedure because of calculation time. The energetic sequences of the isomers may change at larger basis sets, so as many as low-lying isomers in the structural bank are considered. For instance, in optimization of $(Li_2O)_8$, the population size is 30, and the maximum iteration number is 2000. The rate of hitting the global minimum structure is 2/5. After similarity checking[40] of the topological structure, the top 150 lowest energy B3LYP/3-21G isomers in the structural bank are resorted by the single point energy of high level TPSSh/6-311+G*.[41] Finally, the top 30 lowest energy isomers are fully relaxed at TPSSh/6-311+G* level of theory. The number of considered isomers is enough, for example, the top 50 lowest energy B3LYP/3-21G isomers involve all the top 10 lowest energy TPSSh/6-311+G* isomers.

Benchmark calculations

A benchmark calculation on $(Li_2O)_3$ clusters is completed by B3LYP,[36–38] M06,[42] BPW91,[43,44] and TPSSh[41] functionals with 6-311+G* basis set, and the high-level MP2[45] and CCSD(T)[46,47] methods with aug-cc-pVDZ basis set, in addition to zero-point energy (ZPE) at TPSSh/6-311+G*. From Table 1, we can make some conclusions. First, the relative ZPE changes little, so it does not change the energetic sequences of the five isomers. Second, TPSSh functional and MP2 method are consistent with CCSD(T) method in the energetic sequences of the five isomers. The relative energy gaps between TPSSh functional and CCSD(T) method is smallest in this benchmark. As a result, the calculations with TPSSh functional are reliable for $(Li_2O)_n$ clusters.

Table 1. Comparison of computed energies for isomers of $(Li_2O)_3$ clusters (Fig. 2).[a]

Method	Basis set	3A	3B	3C	3D	3E
B3LYP	6–311+g*	−271.232835	−0.05	0.15	0.14	0.29
M06	6–311+g*	−271.084243	−0.04	0.11	0.10	0.33
BPW91	6–311+g*	−271.134809	0.00	0.16	0.15	0.33
MP2	aug-cc-pvdz	−270.318453	0.03	0.15	0.15	0.33
CCSD(T)	aug-cc-pvdz	−270.333268	0.10	0.18	0.18	0.42
TPSSh	6–311+g*	−271.192088	0.10	0.20	0.24	0.49
ZPE	6–311+g*	−271.170092	0.06	0.17	0.20	0.42

[a] Energies for 3A are in atomic units, other energies are relative to this in eV.

Results and Discussion

Geometries

The GA-DFT is applied to the global optimization of $(Li_2O)_n$ ($n = 1$–8) clusters. We locate the global minimum structures and

Table 2. Symmetry, electronic state, binding energy, relative energy, the HOMO–LUMO energy gap, bond number, bond length, and binding energy per Li—O bond of $(Li_2O)_n$ (n = 1–8)clusters.

n	PG[a]	ES[b]	E_b (eV)[c]	E (eV)[d]	ΔE_{HL} (eV)[e]	N_{Li-O}[f]	R_{Li-O}[g] (Å)	E_{Li-O}[h]
1A	$D_{\infty h}$	$^1\sum_g$	−4.61	0.00	2.80	2	1.62	−2.30
1B	C_{2v}	$^3B_1$		2.09		2	1.81	−1.26
2A	D_{2h}	^1A_g	−11.97	0.00	2.66	6	1.63–1.79	−2.00
2B	C_{3v}	$^1A_1$		0.31		7	1.65–1.91	−1.67
3A	C_{2v}	$^1A_1$	−19.45	0.00	1.34	13	1.66–2.07	−1.50
3B	D_{2d}	$^1A_1$		0.11		10	1.63–1.80	−1.94
3C	C_{2v}	$^1A'$		0.20		12	1.64–1.97	−1.60
3D	C_s	$^1A'$		0.24		11	1.64–2.03	−1.75
3E	D_{3h}	$^1A_1'$		0.49		9	1.63–1.79	−2.11
4A	C_s	$^1A'$	−27.57	0.00	1.60	19	1.65–2.00	−1.45
4B	C_{3v}	$^1A_1$		0.10		17	1.67–2.09	−1.62
4C	C_{2h}	^1A_g		0.10		16	1.64–2.02	−1.72
4D	C_{2v}	$^1A_1$		0.15		16	1.64–2.06	−1.71
4E	C_{2v}	$^1A_1$		0.21		18	1.78–2.11	−1.52
4F	C_{2v}	$^1A_1$		0.52		16	1.64–1.96	−1.69
5A	C_s	$^1A'$	−35.96	0.00	3.21	21	1.78–2.00	−1.71
5B	C_{4v}	$^1A_1$		0.05		25	1.66–2.00	−1.44
5C	C_s	$^1A'$		0.14		21	1.66–2.07	−1.71
5D	C_s	$^1A'$		0.15		21	1.77–1.95	−1.71
5E	C_{3v}	$^1A_1$		0.21		22	1.75–1.89	−1.63
5F	C_s	$^1A'$		0.24		22	1.65–1.99	−1.62
6A	C_s	$^1A'$	−44.43	0.00	3.23	31	1.80–2.18	−1.43
6B	C_s	$^1A'$		0.12		28	1.77–2.07	−1.58
6C	C_1	^1A		0.45		28	1.65–2.25	−1.57
6D	C_1	^1A		0.56		27	1.66–2.19	−1.63
7A	C_{2v}	$^1A_1$	−52.72	0.00	3.14	34	1.78–1.98	−1.55
7B	C_s	$^1A'$		0.09		36	1.79–2.15	−1.46
7C	C_1	^1A		0.20		35	1.78–2.13	−1.50
7D	C_s	$^1A'$		0.21		34	1.77–2.19	−1.54
7E	C_1	^1A		0.22		34	1.78–2.09	−1.54
7F	C_1	^1A		0.22		34	1.77–2.12	−1.54
8A	C_1	^1A	−60.91	0.00	3.37	41	1.77–2.22	−1.49
8B	C_1	^1A		0.01		41	1.77–2.21	−1.49
8C	C_s	$^1A'$		0.08		40	1.76–2.18	−1.52
8D	C_2	^1A		0.09		40	1.77–2.10	−1.52
8E	C_s	$^1A'$		0.12		38	1.76–2.12	−1.60
8F	C_1	^1A		0.16		39	1.79–2.05	−1.56

[a] PG: point group. [b] ES: electronic state. [c] E_b: binding energy. [d] E: relative energy. [e] ΔE_{HL}: the HOMO–LUMO energy gap. [f] N_{Li-O}: bond number. [g] R_{Li-O}: bond length. [h] E_{Li-O}: binding energy per Li—O bond.

some relative stable isomers. The structures are indexed in alphabetical order (such as 3A, 3B, 3C, … for $(Li_2O)_3$) by the energy from low to high. The symmetry, electronic state, binding energy, total energy, highest occupied molecular orbital (HOMO), and lowest unoccupied molecular orbital (LUMO) energy gap, Li—O bond number, bond length, and binding energy per Li—O bond of lithium-oxide clusters are listed in Table 2.

Two isomers of $(Li_2O)_1$ clusters are plotted in Figure 2. The ground state 1A is linear, singlet state with $D_{\infty h}$ symmetry, electronic state of $^1\Sigma_g$, Li—O bond length of 1.62 Å. Under the consideration of the triplet excited state, the structure 1B is obtained. 1B is a V-type, triplet state with C_{2v} symmetry, electronic state of $^3B_1$, Li—O bond length of 1.81 Å. 1B is unstable and higher than 1A in energy by 2.09 eV. We predict the reason for the linear structure of 1A is that the structure may have delocalized molecular orbitals (MOs).

$(Li_2O)_2$ clusters (Fig. 2) have a planar global minimum 2A and a three-dimensional (3D) configuration 2B, which are consistent with previous study.[27] 2A is in D_{2h} symmetry, which is composed of a rhombic unit (RU) decorated by two Li atoms at the O corners. 2B is in C_{3v} symmetry, which is higher than 2A by 0.31 eV in energy. Bond number of 2A is 6 and less than the one of 2B. The planar 2A may also have delocalized MOs.

Five isomers of $(Li_2O)_3$ clusters are plotted in Figure 2. 3A and 3B are same with previous study.[27] The global minimum 3A is in C_{2v} symmetry. 3B is in D_{2d} symmetry, which is composed of two vertical RUs. 3C is in C_{2v} symmetry and higher than 3A by 0.20 eV in energy. 3D is in C_s symmetry and higher than 3A by 0.24 eV in energy. 3E is a planar structure with a six-membered ring and has a high symmetry (D_{3h}), but is poor in stability.

Six isomers of $(Li_2O)_4$ clusters are plotted in Figures 2. 4C and 4D are same with previous study.[27] The global minimum structure is 4A in this study, but the ground state in previous study is 4D. 4A is in C_s symmetry and the O atoms are located at the corners of a flattened tetrahedron and its right half part has a close resemblance with 4C. 4B has a high symmetry (C_{3v}), which has a tetrahedral unit (TU) plus one Li. In a TU, there are four O in the vertices, six Li in the edges, and one Li in the central. 4C is in C_{2h} symmetry and the O atoms lie in a plane. It is close to 4B in energy and composed of five RUs. 4D is in C_{2v} symmetry and the O atoms are at the corners of a regular tetrahedron. 4E is in C_{2v} symmetry and the O atoms lie in a plane. 4F (C_{2v}) is an eversion of 4C (C_{2h}) and the eversion changes the symmetry and makes energy higher by 0.42 eV.

Six isomers of $(Li_2O)_5$ clusters are listed in Figures 3. 5A is in C_s symmetry and it is a close shell structure (CSS). In a CSS, each Li is bonded with at least two O. 5B is in C_{4v} symmetry

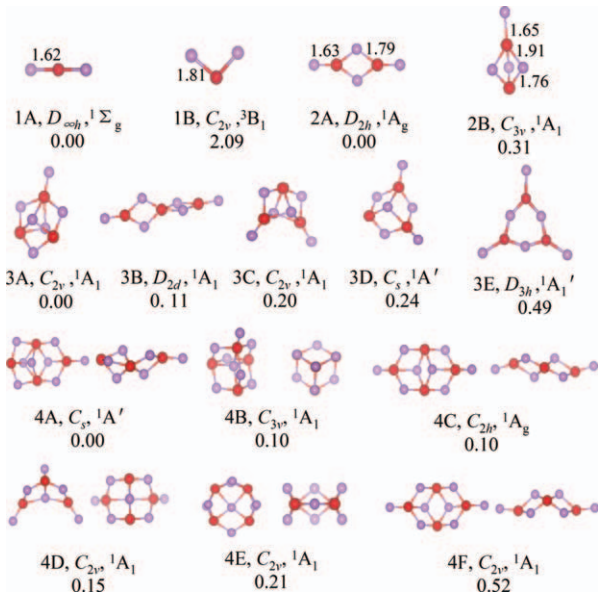

Figure 2. The global minimum and low-energy isomers for $(Li_2O)_n$ (n = 1–4) clusters at the TPSSh/6-311+G* level. Labeled are the point groups, electronic state and relative energies in eV. Li purple, O red. [Color figure can be viewed in the online issue, which is available at wileyonlinelibrary.com.]

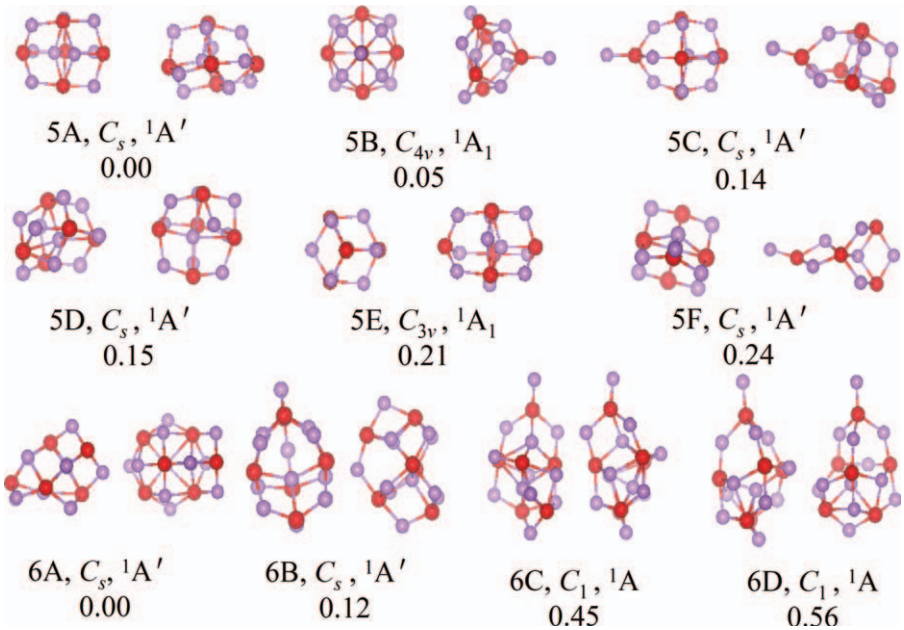

Figure 3. The global minimum and low-energy isomers for $(Li_2O)_n$ (n = 5–6) clusters at the TPSSh/6-311+G* level. [Color figure can be viewed in the online issue, which is available at wileyonlinelibrary.com.]

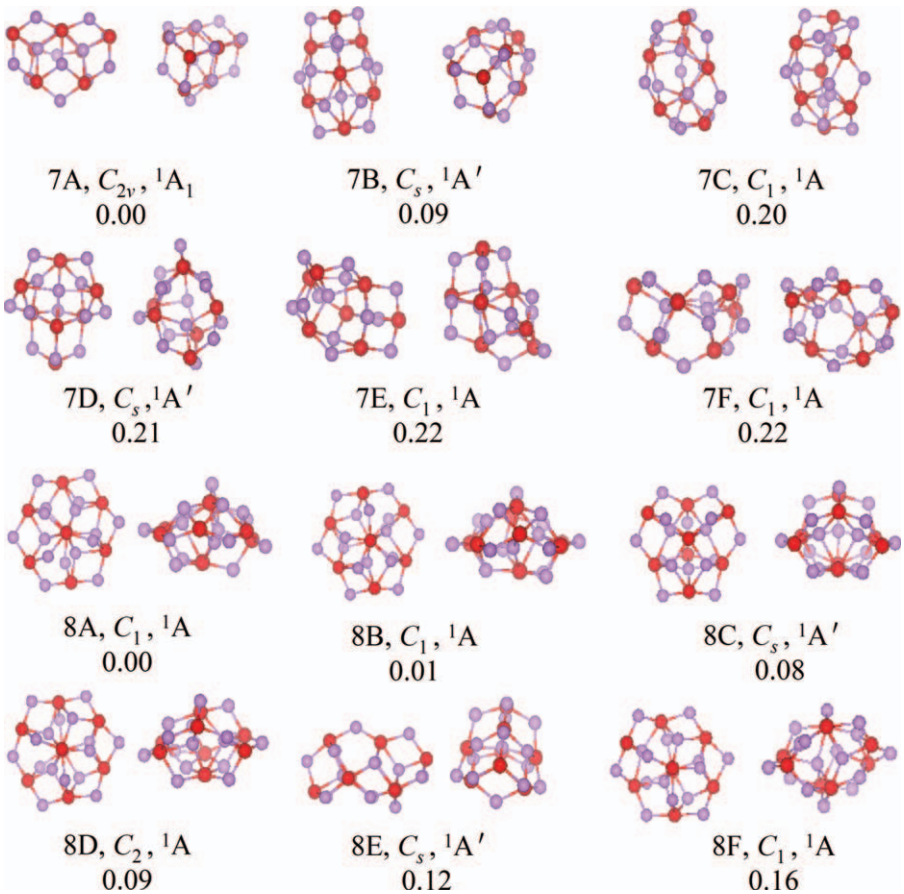

Figure 4. The global minimum and low-energy isomers for $(Li_2O)_n$ (n = 7–8) clusters at the TPSSh/6-311+G* level. [Color figure can be viewed in the online issue, which is available at wileyonlinelibrary.com.]

and the O atoms are located at the corners of a tetragonal pyramid. The structure of 5B is defined as C_{4v} structural unit. One inner Li of 5A is moved outer of the structure to form 5C (C_s). 5C is an open shell structure (OSS). In an OSS, there is at least one Li bonded with only one O. 5D is in C_s symmetry and higher than 5C only 0.01 eV in energy. 5E is in C_{3v} symmetry, which is composed of two TUs, but it is too strained and not stable. 5F (C_s) is an union of 4B and 4C, that is, TU plus RU.

Four types of geometries of $(Li_2O)_6$ clusters are plotted in Figure 3. The global minimum 6A is C_s symmetry, which is an union of a TU and a C_{4v} structural unit. It is also the global minimum in previous study.[27] 6B is C_s symmetry and has one TU, which is same with that in the previous study.[27] 6C (C_1) and 6D (C_1) both are OSS and are much higher than the former CSS in energy. Thus, we can conclude that a CSS is more stable than an OSS at cluster size $n \geq 6$.

To $(Li_2O)_7$ clusters (Fig. 4), we list six geometries. The ground state 7A has a higher symmetry (C_{2v}) and it is composed of two TUs and a C_{4v} structural unit. 7B is in C_s symmetry and has a TU. 7C is in C_1 symmetry and higher than 7A by 0.20 eV in energy. 7D is in C_s symmetry and it has a TU. 7E is in C_1 symmetry and it has two TUs. 7F is in C_1 symmetry and it is very close to 7E in energy.

In the structures of $(Li_2O)_8$ clusters (Fig. 4), 8A (C_1) has one TU. 8B is in C_1 symmetry. 8C (C_s) has two TUs, which looks like a butterfly. 8D is in C_2 symmetry. The first four isomers (8A, 8B, 8C, and 8D) are within 0.09 eV in energy and they all can be global minimum. 8E (C_s) is composed of two TUs. 8F is in C_1 symmetry and higher than 8A by 0.16 eV in energy. 8A, 8B, 8D, and 8F are like the changed shape of butterfly. 8F is a distortion of 8C, where the distortion breaks the symmetry from C_s to C_1 and makes energy higher by 0.08 eV.

From what has been discussed above, we can conclude that the structure of cluster will become more complex as cluster size increases. At $n \leq 4$, the global minimum structures are open shell in geometry, that is, there are Li atoms bonded with only one O atom. However, the structures are close shell at $n \geq 5$. The stable CSSs usually have a TU. In a TU, the central Li atom is bonded with four O atoms, which is very different from bulk lithium-oxide, where each Li atom is bonded with eight O

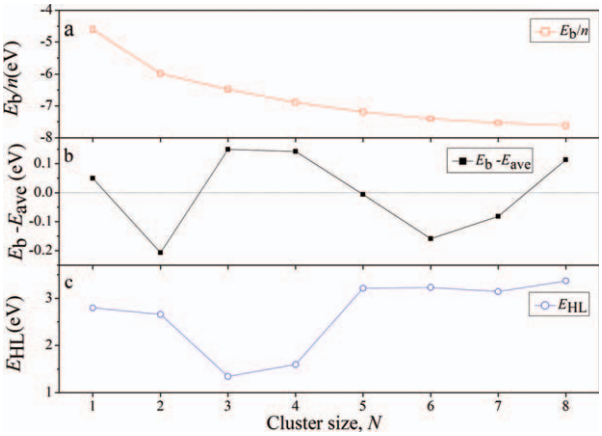

Figure 5. The dependence of binding energy per Li_2O unit E_b/n (**a**) of the ground state in $(Li_2O)_n$ clusters as cluster size n and binding energy of the global minima of lithium oxide clusters relative to E_{ave} (**b**), a fit to the binding energies of the global minima at size ratio of $1 \leq n \leq 8$ using the form $-9.0768 + 20.83429*n^{1/3} - 9.42675*n^{2/3} - 6.98794*n$, which represents the average energy of the global minima. The dependence of HOMO–LUMO energy gaps E_{HL} (**c**) of the ground state in $(Li_2O)_n$ (n = 1–8) clusters as a function of the cluster size n. [Color figure can be viewed in the online issue, which is available at wileyonlinelibrary.com.]

atoms. Comparing with other 1–2 nanoclusters (SiO_2, TiO_2, ZrO_2, and MgF_2), the global minimum structures of $(Li_2O)_n$ clusters are in agreement with the ones of $(SiO_2)_n$[15–19] clusters at $n = 1$, $n = 2$, and $n = 3$, and the global minimum structures of $(SiO_2)_n$ clusters are open shell in geometry. For $(TiO_2)_n$[16,20–22] and $(ZrO_2)_n$[20,23–25] clusters, the open shell to close shell structural transition occurs at $n = 8$. The global minimum structures of $(Li_2O)_n$ clusters are consistent with the ones of $(MgF_2)_n$[48] clusters at $n = 1$, $n = 2$, and $n = 3$, and the open shell to close shell structural transition occurs at $n = 9$ for $(MgF_2)_n$ clusters with a semiempirical method.

Binding energies and stability

In this part, we analyze the binding energies and stability of the ground state structures of $(Li_2O)_n$ (n = 1–8) clusters. The dependence of the binding energy per Li_2O unit of $(Li_2O)_n$ clusters (E_b/n) and the difference ($E_b - E_{ave}$) between binding energy and average energy as a function of the cluster size n are shown in Figures 5a and 5b. The binding energy E_b is defined as:

$$E_b = E_{clust} - 1/2 * E(O_2) * N_O - E(Li) * N_{Li} \quad (1)$$

where $E(O_2)$ and $E(Li)$ are the energies of O_2 molecule and Li atom, respectively; E_{clust} is the total energy of the cluster; N_O and N_{Li} represent the number of O and Li, respectively. Figure 5a shows that the binding energy per Li_2O unit decreases with cluster size n. Moreover, the energies are depicted in Figure 5b in a manner that emphasizes particular stable minima or "magic numbers." Note that the binding energy is lower than the average when $n = 2$, 6, and 7, so it can be concluded that the ground states of $(Li_2O)_2$, $(Li_2O)_6$, and $(Li_2O)_7$ clusters are most stable "magic numbers". 2A and 7A have high geometric symmetry, where the former may be stabilized by the delocalized π MOs, and the stability of the later may due to the two TUs. 6A has stable structural units of TU and C_{4v} which may lead to the stability.

Electronic structure

Here, we only analyze the electronic structures of the ground state. The HOMO–LUMO energy gap (ΔE_{HL}) of cluster is an important quantity related to the stability of $(Li_2O)_n$ clusters. As shown in Figure 5c, the HOMO–LUMO energy gaps at $n \leq 4$ are lower than the ones at $n \geq 5$, we believe the reason is that the structures are open shell at $n \leq 4$ and the structures are close shell at $n \geq 5$.

Moreover, we find that some electronic structures of $(Li_2O)_n$ clusters are very particular. Because Li atom is bonded with O atom by ionic bond, so it is difficult to analyze by Lewis bonding theory. As a result, we apply a new tool named adaptive natural density partitioning (AdNDP) for obtaining patterns of chemical bonding. The method was recently developed by Zubarev and Boldyrev.[49] AdNDP is based on the concept of the electron pair as the main element of chemical bonding models, which recovers both Lewis bonding elements (1c–2e and 2c–2e objects) and delocalized bonding elements (nc–2e). Because 1A is a linear structure, 2A and 3E are planar structures and 4B has a TU, so we analyze the electronic structures of 1A, 2A, 3E, and 4B by AdNDP. The results of the AdNDP analysis are plotted in Figure 6.

There are 2c–2e σ bonds (with occupancy number ON = 1.99 $|e|$) and two 3c–2e π bonds (ON = 2.00 $|e|$) in 1A (Fig. 6a). 2A (Fig. 6b) consists of six σ bonds and two 6c-2e π bonds (ON = 2.00 $|e|$). The σ bonding is represented as a combination of two 2c–2e σ bonds (ON = 1.99 $|e|$, superimposed on the single molecular framework), two 3c–2e σ bonds (ON = 1.99 $|e|$, superimposed on the single molecular framework) and two 6c–2e σ bonds (ON = 2.00 $|e|$). 3E (Fig. 6c) includes nine σ bonds and three delocalized 9c–2e π bonds (ON = 2.00 $|e|$). The σ bonding is represented as a combination of three 2c–2e σ bonds (ON = 1.96 $|e|$, superimposed on the single molecular framework), three 3c–2e σ bonds (ON = 1.99 $|e|$, superimposed on the single molecular framework), and three 9c–2e σ bonds (ON = 2.00 $|e|$). However, the planar structure 3E is very poor in stability. 4B (Fig. 6d) includes four 2c–2e σ bonds (ON = 1.95–1.94 $|e|$) and 12 4c–2e σ bonds (ON = 1.99–1.96 $|e|$). The probability of the Li atom in the center of 4B participating in the bonding is higher than others, which may lead to the charge of central Li lower.

In addition, 2A has four π-electrons. According to the $(4n+2)$ Hückel's rule, 2A should be antiaromatic. Nucleus-independent chemical shifts (NICS)[50] value is a popular measurement for aromaticity (negative NICS values mean aromaticity and positive NICS values mean antiaromaticity). However, NICS value at the center reveals that 2A is aromatic (NICS = −3.80 ppm) comparing to benzene (NICS = −8.19 ppm), which may be due to the effect of the σ bonds.

Unique charge of the central lithium

We find that mulliken charges of some central lithium atoms are very high up to about +5.0 e, which is wrong. As we

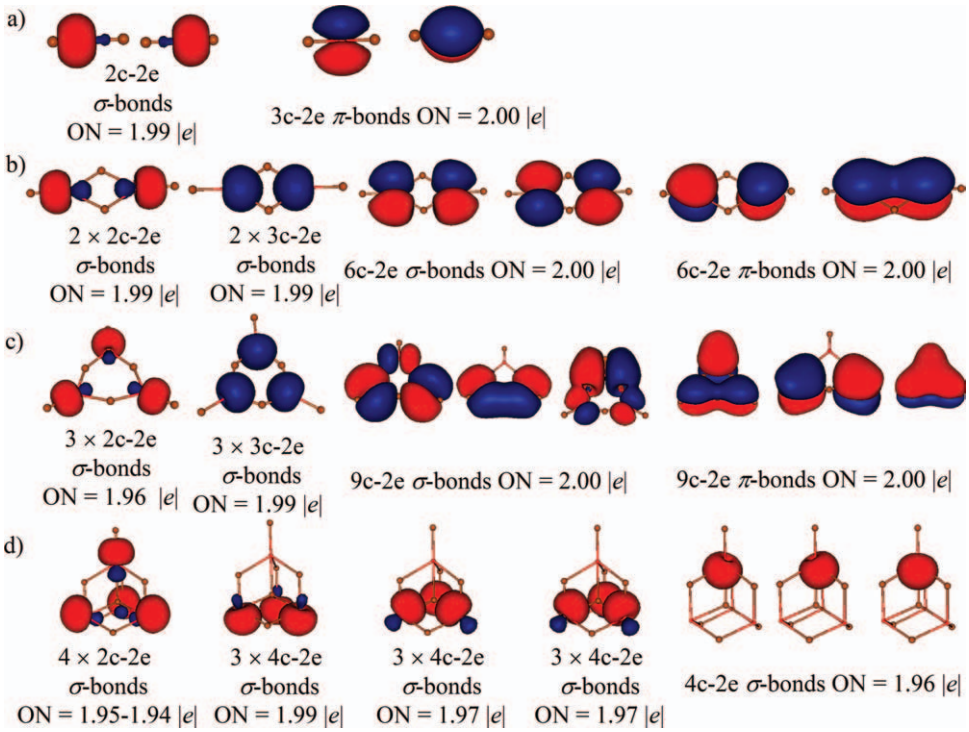

Figure 6. The results of the AdNDP localization for 1A (**a**), 2A (**b**), 3E (**c**), and 4B (**d**), respectively (molecular visualization was performed using MOLEKEL 5.4). [Color figure can be viewed in the online issue, which is available at wileyonlinelibrary.com.]

know, the charge of lithium atom should be near +1.0 *e*. Next, we analyze natural charge of lithium atom by natural population analysis (NPA). The dependence of charges as cluster size is shown in Figure 7 (the ground states of $(Li_2O)_n$ clusters). From this graph, we see that the maximum natural charge

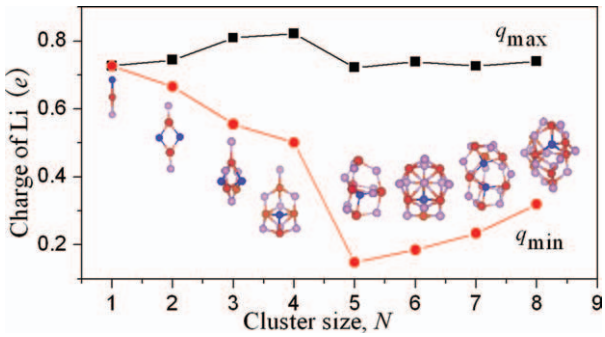

Figure 7. The dependence of natural charge as cluster size, the maximum charge q_{max} (the minimum charge q_{min}) in black (red) line representation, the central lithium atom in blue ball representation. [Color figure can be viewed in the online issue, which is available at wileyonlinelibrary.com.]

(q_{max}) is close to the minimum one (q_{min}) when $n \leq 4$, the maximum is +0.82 *e* and the minimum is +0.50 *e* at $n = 4$. However, q_{min} decreases rapidly when *n* is 5, especially the one is extremely low at $n = 5$, which is +0.15 *e* far from +1.0 *e*, and q_{min} is also much less than +1.0 *e* at $n = 6$–8. It is found that the Li atom with extremely low charge is in the center of the TU. But why it happened? We suggested that Li element has a large *sp* interaction due to the lack of *p* orbital in the core. When the structure has a TU, the central Li atom in the TU is interacted with four O atoms, so the central Li atom is in sp^3 interactions and the lone-pair electrons of O is filled with the four vacant sp^3 orbitals of Li. Such a unique charge transformation leads to the unusual low positive charge of the central Li. Similar charge transformation is viewed in lithium clusters, where electrons are also transformed to the central Li.[51] The central Li atom is sp^3 interactions by NPA for 4B, 5A, and 6A, and so forth. 4B has a TU but is not the global minimum, and the natural charge of the central Li in 4B is also very low in +0.16 *e*. The reason is Li atom in the center of 4B participating in the bonding is higher than others.

Discussion of global optimization methods

There are 24 atoms in $(Li_2O)_8$ clusters. If using an empirical/semiempirical method, 24 atoms is not a challenging cluster size, but it is very difficult for GA-DFT method, and the calculation time for larger clusters becomes intolerable. To study larger size of $(Li_2O)_n$ clusters, it is better to combine an empirical/semiempirical method with DFT method. Our GA is not a standard one, where the Deaven-Ho crossover[39] is adapted and the offspring is generated one by one instead of generations. Such a method is better classified as evolutional algorithm. However, to be consistent with the literatures,[52,53] we still named our method as "genetic algorithm".

GA used in this work is one of the most applicable global search tools, but its performance is not so high for structural optimization problems. There are some newly developed structural global optimization methods with much higher performance than GA. For example, the funnel-hopping method[54] is much faster than GA when applied to the optimization of the benchmark problems, Lennard–Jones clusters. As we know, the "basin-hopping"[55] is a two-phase global optimization method, that is, global optimization (GO) phase plus local optimization (LO) phase. Most successful cluster global optimization methods, such as GA, simulated annealing,[56] and so forth, can be taken as basin-hopping in concept. However, in the "funnel-hopping" method, by inserting the cluster surface smoothing approach into the gradient-based LO-phase and the GO-phase as a second LO-phase, the GO-phase can focus on the global information of the PES over the various funnels. The "funnel-hopping" method can locate global minima of clusters with much lower costs compared to the basin-hopping methods, but is much more complex and hardly combined with DFT. For the global search of *ab initio* PES for larger cluster size, a more efficient global search method (such as funnel-hopping) should be

adopted directly combined with DFT method, which is the goal of our group in the near future.

Conclusions

Theoretical properties of stoichiometric lithium-oxide clusters $(Li_2O)_n$ ($n = 1$–8) have been studied by means of GA, in conjunction with DFT, relying on B3LYP and TPSSh functionals. We analyze the geometry, binding energy, electronic structure, some unique charge of the central lithium and make some conclusions. (i) In $(Li_2O)_n$ ($n = 1$–8) clusters, the planar structures are global minimum up to $n = 2$, but the structures of clusters are all 3D at $n \geq 3$. It can be seen as cluster size increases, the structures of cluster are more complex. (ii) The most stable structure is obtained at low spin multiplicity. (iii) The global minimum structures of $(Li_2O)_2$, $(Li_2O)_6$, and $(Li_2O)_7$ clusters are more stable than the others. Because the ground state of $(Li_2O)_2$ clusters has delocalized MOs, so the electronic structure is very stable. The ground state of $(Li_2O)_6$ has stable structural units of tetrahedral and C_{4v}. The ground state of $(Li_2O)_7$ clusters is composed of two TUs and a C_{4v} structural unit, so the geometry is very stable. (iv) The natural charge of central lithium atom is lower because of charge transfer. The natural charges of the central lithium in 4B, 5A, and 6A, and so forth are relative low and the reasons are as follows: their structures have the TU where the central lithium is connected with four oxygen atoms and the large *p* orbital of Li leads to unexpected stable structures. Besides, the probability of the Li atom in the center of 4B participating in the bonding is higher than others. (v) In crystal Li_2O, each Li is bonded with eight O and each O is bonded with four Li. However, for $(Li_2O)_n$ clusters, the Li is bonded with four O in the TU.

Acknowledgment

The calculations are carried out on the High-Performance Computing Center of Anhui University.

Keywords: lithium-oxide cluster · genetic algorithm · density functional theory · geometric optimization · charge transformation

How to cite this article: Y. Yuan L. Cheng, *Int. J. Quantum Chem.* **2013,** *113*, 1264–1271. DOI: 10.1002/qua.24274

[1] F. Baletto, R. Ferrando, *Rev. Mod. Phys.* **2005**, *77,* 371.
[2] P. J. Ziemann, A. W. Castleman, *Phys. Rev. B* **1991**, *44,* 6488.
[3] J. M. Recio, R. Pandey, *Phys. Rev. A* **1993**, *47,* 2075.
[4] J. M. Recio, A. Ayuela, R. Pandey, A. B. Kunz, *Z. Phys. D: At. Mol. Clust.* **1993**, *26,* 237.
[5] E. de la Puente, A. Aguado, A. Ayuela, J. M. Lopez, *Phys. Rev. B* **1997**, *56,* 7607.
[6] C. Roberts, R. L. Johnston, *Phys. Chem. Chem. Phys.* **2001**, *3,* 5024.
[7] X. H. Liu, X. G. Zhang, *Gen. Introd. Chem.* **1997**, *101,* 1071.
[8] T. P. Martin, T. Bergmann, Malinowski, N. *J. Chem. Soc. Faraday Trans.* **1990**, *86,* 2489.
[9] V. Boutou, M. A. Lebeault, A. R. Allouche, C. Bordas, F. Pauling, J. Viallon, J. Chevaleyre, *Phys. Rev. Lett.* **1998**, *80,* 2817.
[10] Q. Wang, Q. Sun, J. Z. Yu, B. L. Gu, Y. Kawazoe, *Phys. Rev. A* **2000**, *62,* 3203.
[11] V. Boutou, M. A. Lebeault, A. R. Allouche, F. Pauling, J. Viallon, C. Bordas, J. Chevaleyre, *J. Chem. Phys.* **2000**, *112,* 6228.
[12] G. Chen, Z. F. Liu, X. G. Gong, *J. Chem. Phys.* **2004**, *120,* 8020.
[13] H. Limberger, T. Martin, *Z. Phys. D: At. Mol. Clust.* **1989**, *12,* 439.
[14] A. Albu-Yaron, T. Arad, M. Levy, R. Popovitz-Biro, R. Tenne, J. M. Gordon, D. Feuermann, E. A. Katz, M. Jansen, C. Muehle, *Adv. Mater.* **2006**, *18,* 2993.
[15] R. Zhang, W. Fan, *J. Clust. Sci.* **2006**, *17,* 541.
[16] C. R. A. Catlow, S. T. Bromley, S. Hamad, M. Mora-Fonz, A. A. Sokol, S. M. Woodley, *Phys. Chem. Chem. Phys.* **2010**, *12,* 786.
[17] E. Flikkema, S. T. Bromley, *J. Phys. Chem. B* **2004**, *108,* 9638.
[18] T. Chu, R. Zhang, H. Cheung, *J. Phys. Chem. B* **2001**, *105,* 1705.
[19] S. T. Bromley, F. Illas, *Phys. Chem. Chem. Phys.* **2007**, *9,* 1078.
[20] S. Woodley, S. Hamad, J. Mejias, C. Catlow, *J. Mater. Chem.* **2006**, *16,* 1927.
[21] Z. Qu, G. J. Kroes, *J. Phys. Chem. B* **2006**, *110,* 8998.
[22] S. Hamad, C. Catlow, S. Woodley, S. Lago, J. Mejias, *J. Phys. Chem. B* **2005**, *109,* 15741.
[23] S. M. Woodley, S. Hamad, C. R. A. Catlow, *Phys. Chem. Chem. Phys.* **2010**, *12,* 8454.
[24] S. Li, D. A. Dixon, *J. Phys. Chem. A* **2010**, *114,* 2665.
[25] S. Chen, Y. Yin, D. Wang, Y. Liu, X. Wang, *J. Cryst. Growth* **2005**, *282,* 498.
[26] C. Bréchignac, P. Cahuzac, F. Carlier, M. de Frutos, J. Leygnier, J. P. Roux, *J. Chem. Phys.* **1993**, *99,* 6848.
[27] F. Finocchi, C. Noguera, *Phys. Rev. B* **1996**, *53,* 4989.
[28] F. Finocchi, T. Albaret, C. Noguera, *Farad. Dis.* **1997**, *106,* 233.
[29] J. Viallon, M. A. Lebeaulta, F. Lepine, J. Chevaleyre, C. Jonin, A. R. Allouche, M. Aubert-Frecon, *Eur. Phys. J. D* **2005**, *33,* 405.
[30] P. Goel, N. Choudhury, S. L. Chaplot, *Pramana-J. Phys.* **2004**, *63,* 409.
[31] L. Mitas, J. C. Grossman, I. Stich, J. Tobik, *Phys. Rev. Lett.* **2000**, *84,* 1479.
[32] D. E. Bacelo, R. Binning, Jr., Y. Ishikawa, *J. Phys. Chem. A* **1999**, *103,* 4631.
[33] D. Tian, H. Zhang, J. Zhao, *Solid State Commun.* **2007**, *144,* 174.
[34] A. N. Alexandrova, A. I. Boldyrev, *J. Chem. Theory Comput.* **2005**, *1,* 566.
[35] M. J. Frisch, G. W. Trucks, H. B. Schlegel, G. E. Scuseria, M. A. Robb, J. R. Cheeseman, G. Scalmani, V. Barone, B. Mennucci, G. A. Petersson, H. Nakatsuji, M. Caricato, X. Li, H. P. Hratchian, A. F. Izmaylov, J. Bloino, G. Zheng, J. L. Sonnenberg, M. Hada, M. Ehara, K. Toyota, R. Fukuda, J. Hasegawa, M. Ishida, T. Nakajima, Y. Honda, O. Kitao, H. Nakai, T. Vreven, J. A. Montgomery, Jr., J. E. Peralta, F. Ogliaro, M. Bearpark, J. J. Heyd, E. Brothers, K. N. Kudin, V. N. Staroverov, R. Kobayashi, J. Normand, K. Raghavachari, A. Rendell, J. C. Burant, S. S. Iyengar, J. Tomasi, M. Cossi, N. Rega, J. M. Millam, M. Klene, J. E. Knox, J. B. Cross, V. Bakken, C. Adamo, J. Jaramillo, R. Gomperts, R. E. Stratmann, O. Yazyev, A. J. Austin, R. Cammi, C. Pomelli, J. W. Ochterski, R. L. Martin, K. Morokuma, V. G. Zakrzewski, G. A. Voth, P. Salvador, J. J. Dannenberg, S. Dapprich, A. D. Daniels, O. Farkas, J. B. Foresman, J. V. Ortiz, J. Cioslowski, D. J. Fox, Gaussian 09, revision B. 01; Gaussian: Wallingford, CT, **2009**.
[36] A. D. Becke, *J. Chem. Phys.* **1993**, *98,* 5648.
[37] C. Lee, W. Yang, R. G. Parr, *Phys. Rev. B* **1988**, *37,* 785.
[38] B. Miehlich, A. Savin, H. Stoll, H. Preuss, *Chem. Phys. Lett.* **1989**, *157,* 200.
[39] D. M. Deaven, K. M. Ho, *Phys. Rev. Lett.* **1995**, *75,* 288.
[40] L. J. Cheng, W. S. Cai, X. G. Shao, *Chem. Phys. Lett.* **2004**, *389,* 309.
[41] T. Tao, J. P. Perdew, V. N. Staroverov, G. E. Scuseria, *Phys. Rev. Lett.* **2003**, *91,* 146401.
[42] Y. Zhao, D. G. Truhlar, *J. Chem. Phys.* **2006**, *125,* 194101.
[43] W. B. Smith, *Magn. Reson. Chem.* **1999**, *37,* 103.
[44] J. P. Perdew, J. A. Chevary, S. H. Vosko, K. A. Jackson, M. R. Pederson, D. J. Singh, C. Fiolhais, *Phys. Rev. B* **1993**, *48,* 4978.
[45] M. Feyereisen, G. Fitzgerald, A. Komornicki, *Chem. Phys. Lett.* **1993**, *208,* 359.
[46] P. Hobza, H. L. Selzle, E. W. Schlag, *J. Phys. Chem.* **1996**, *100,* 18790.
[47] P. R. Schreiner, A. A. Fokin, R. A. Pascal, Jr., A. De. Meijere, *Org. Lett.* **2006**, *8,* 3635.
[48] E. Francisco, A. M. Pendas, M. Blanco, *J. Chem. Phys.* **2005**, *123,* 234305.
[49] D. Yu. Zubarev, A. I. Boldyrev, *Phys. Chem. Chem. Phys.* **2008**, *10,* 5207.

[50] P. v. R. Schleyer, C. Maerker, A. Dransfeld, H. Jiao, N. J. R. v. E. Hommes, *J. Am. Chem. Soc.* **1996**, *118,* 6317.
[51] I. Boustani, W. Pewestorf, *Phys. Rev. B* **1987**, *35,* 9437.
[52] B. Hartke, *J. Phys. Chem.* **1993**, *97,* 9973.
[53] C. Roberts, R. L. Johnston, *Phys. Chem. Chem. Phys.* **2001**, *3,* 5024.
[54] L. J. Cheng, Y. Feng, J. Yang, J. L. Yang, *J. Chem. Phys.* **2009**, *130,* 214112.
[55] J. David, J. P. K. Doye, *J. Phys. Chem. A* **1997**, *101,* 5111.
[56] S. Kirkpatrick, C. D. Gelatt, Jr., M. P. Vecchi, *Science* **1983**, *220,* 671.

Received: 14 March 2012
Revised: 24 May 2012
Accepted: 20 June 2012
Published online on 12 July 2012